IT'IS FOUNDATION

Foundation for Research on Information Technologies in Society

Prof. Dr. Niels Kuster

Director, IT'IS Foundation
Professor, Swiss Federal Institute of Technology – ETH Zurich
Phone +41 44 245 9690 · kuster@itis.swiss

Verification Report Dipoles001AA201903

System Validation Dipoles from 3900 MHz to 4900 MHz

Andreas Christ and Niels Kuster

Issued: Zurich, March 25, 2019

Contents

1 Introduction and Objectives

For the upcoming revision of [1], additional frequencies in the range from 3.9 GHz to 4.9 GHz are introduced for system check and system validation to cover the 5G sub-6-GHz (sub6) frequencies. Four new dipole antennas with nominal frequencies of 3.9 GHz, 4.2 GHz, 4.6 GHz, and 4.9 GHz were defined. The incorporation of these new antennas and the corresponding numerical specific absorption rate (SAR) targets into [1] requires that these target values be independently verified both numerically and experimentally.

The objectives of this report are to document:

- the newly developed dipoles and their corresponding CAD files
- the target values for 1 g psSAR, 10 g psSAR, peak SAR, and local SAR at 20 mm offset from the dipole axis normalized to 1 W forward power
- uncertainty budget of the target values
- numerical verification of the target values by an independent laboratory under the condition that all differences are less than the combined uncertainty of both numerical evaluations
- experimental verification of the target values by an independent laboratory with physical dipoles and application of instrumentation and procedures compliant with [1] under the condition that all differences are well within the combined uncertainty of the numerical assessment and the experimental evaluation

2 CAD Models

2.1 Numerical Dipole Models

Numerical dipole models are developed for the system validation antennas – D3900V2 and D4600V2 – with nominal frequencies of 3.9 GHz and 4.6 GHz, respectively, and two new antennas – D4200V0 and D4900V0 – with nominal frequencies of 4.2 GHz and 4.9 GHz, respectively. The mechanical characteristics of the antennas are given in Table 1. The dipole legs are mounted on a shorting cylinder with a diameter of 14 mm and a length of 30 mm (Section 3.2).

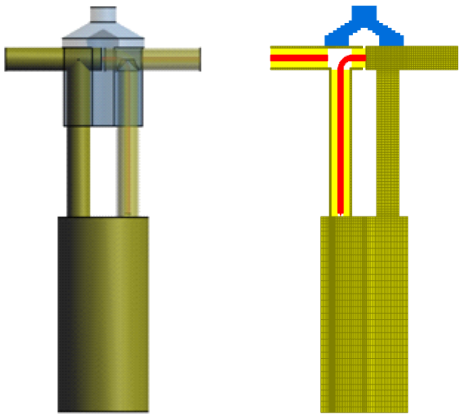

Figure 1: CAD model of the 4.2 GHz dipole antenna (left) and discretized view of the antenna's center cross section (right); gold: perfect electric conductors, yellow: dielectrics of the coaxial cables, red: conductors of the coaxial cables, blue: spacer.

Because the frequencies are higher than those reported in [2], the dipoles are modeled with the 50 Ω coaxial feed line in one leg. The coaxial line is terminated with an edge source at the shorting cylinder at the bottom of the leg. Since the edge source and the diameter of the coaxial line are electrically small,

Table 1: Mechanical characteristics of the dipoles.

Model	Arm length (over all) [mm]	Leg length [mm]	Caps	Arm diameter [mm]	Leg diameter [mm]
D3900V2	32.0	21.0	-	3.6	3.6
D4200V0	30.1	22.5	-	3.6	3.6
D4600V2	27.0	21.7	⌀4.5 mm × 5.0 mm	3.6	3.6
D4900V0	25.0	19.1	⌀4.5 mm × 5.0 mm	3.6	3.6

transverse electromagnetic (TEM) mode becomes established in the coaxial cable after a few mesh cells, and the reflection coefficient can be calculated directly from the feed-point impedance of the edge source.

For precise positioning, the dipoles are equipped with a dielectric spacer. As the impact of the spacer on the SAR at frequencies above 3 GHz needs to be considered, this is integrated into the numerical models. The dielectric parameters of the spacer and the coaxial feed line are given in Table 2. All metal parts are modeled as perfect electric conductors.

Table 2: Dielectric parameters of the dipole and phantom models. All dielectric parts except for the tissue simulating liquid (TSL) are lossless and assumed to be independent of the frequency.

Part	Relative permittivity ϵ_r
Dielectric of inner conductor	2.07
Spacer	2.53
Phantom shell	3.7
Head TSL	see [1]

2.2 Flat Phantom

The flat phantom is modeled as a parallelepiped of 150 mm height that terminates in free space with dielectric parameters as defined in [1]. It is simulated with a reduced cross section of $180 \times 120\,\text{mm}^2$, which corresponds to the required minimum dimensions according to [2]. The bottom of the flat phantom consists of a lossless dielectric shell of 2.0 mm thickness. The dielectric parameters of the shell are given in Table 2.

3 Methods

3.1 Numerical Methods

All numerical evaluations were carried out with the finite-difference time-domain solver [3] of the simulation platform Sim4Life, Versions 4.0 and 4.4 (ZMT Zurich MedTech AG, Switzerland). The psSAR is evaluated by direct integration of the local SAR in cubical volumes of the respective dimensions centered above the dipole feed points. Sim4Life and GNU Octave were used [4] for further post-processing.

3.2 Modeling Parameters and Simulation Settings

In addition to the description of the simulation settings in [2], the following considerations are required to be able to obtain consistent results at frequencies above 3 GHz:

- The mesh step for discretization of the cross sections of the coaxial lines is limited to 0.2 mm and to 0.5 mm.
- The mesh step for the discretization of the spacer and of the phantom shell in direction normal to the liquid surface is limited to 0.4 mm.

- The bottom end of the shorting cylinder terminates in absorbing boundary conditions.

3.3 Experimental Methods

The experimental evaluation of the SAR values is carried out with the dosimetric assessment systems DASY52 and DASY6 (Schmid & Partner Engineering AG, Switzerland). The dipoles are measured with the elliptical flat phantom defined in [1], according to the adapted ISO 17025 accredited calibration protocol for dipoles.

4 Results

4.1 Numerical Target Values

Table 3 shows the numerical results of the 1 g psSAR, the 10 g psSAR, the peak SAR and the local SAR at an offset 20 mm from the dipole axis according to the specifications of [1]. The SAR target values are normalized to a forward power of 1 W.

Table 3: SAR target values for the dipoles defined in Seciton 2.1. All results are normalized to 1 W forward power.

Frequency [MHz]	**1 g psSAR [W/kg]**	**10 g psSAR [W/kg]**	**peak SAR [W/kg]**	**20 mm SAR [W/kg]**
3900	67.5	23.3	193.5	13.3
4200	66.4	22.2	200.9	14.6
4600	66.7	21.5	220.0	16.8
4900	68.4	21.2	242.0	17.9

4.2 Numerical Uncertainty Budget

4.2.1 General

The evaluation of the numerical uncertainty budget is according to the specifications of [5] and has been adapted to the particular requirements of the dipole antennas as described in Section 2. The expanded numerical uncertainty ($k = 2$) has been assessed as 0.3 dB. The complete uncertainty budget is given in Table 4, and details can be found in the following sections. All tolerances have been derived for 1 g psSAR, the 10 g psSAR, the peak SAR and the 20 mm SAR. For a conservative uncertainty budget, the respective maximum tolerance is chosen (Table 4).

4.2.2 Mesh Resolution of the Phantom

For the assessment of the uncertainty in mesh resolution of the phantom, the maximum mesh steps for the discretization of the phantom and of the area of the psSAR are increased and divided by 2. The difference reported is based on the assumption of a normal distribution.

4.2.3 Mesh Resolution of the Dipole

For the assessment of the uncertainty in mesh resolution of the dipole antennas, the maximum mesh step in the antenna region is divided by 2. The difference reported is based on the assumption of a normal distribution.

4.2.4 Positioning

The distance between the phantom and the dipole has been increased and decreased by one maximum mesh step in the antenna region (0.2 mm). The difference reported is based on the assumption of a rectangular distribution.

4.2.5 Phantom Dimensions

The impact of the reduced phantom size is evaluated by increasing its default cross section of $180 \times 120\,\text{mm}^2$ by a factor of two in both directions. The difference reported is based on the assumption of a rectangular distribution.

4.2.6 Shorting Cylinder

As the shape and size of the generic shorting cylinder of the model deviate slightly from the design of the manufactured dipoles, the dependence of the psSAR on diameter and length is evaluated. With the cylinder terminating in absorbing boundary conditions, the impact of length on the SAR is negligible. The dependence on the cylinder radius is reported for an uncertainty of 1 mm.

4.2.7 Power Budget and Convergence

The power budget is evaluated, and the deviation from 100% is reported. The convergence uncertainty is determined according to [5]. Rectangular distribution is assumed in both cases.

Table 4: Numerical uncertainty budget according to [5].

Unc. component	**Tolerance [dB]**	**Prob. Distr.**	**Div.**	c_i	**Std. Unc.**	ν_i **or** ν_eff
Mesh resolution phantom	0.07	N	1	1	0.07	∞
Mesh resolution dipole	0.11	N	1	1	0.11	∞
Positioning (dist. dipole to phantom)	0.11	R	$\sqrt{3}$	1	0.06	∞
Phantom dimensions	0.04	R	$\sqrt{3}$	1	0.02	∞
Shorting cylinder	0.02	N	1	1	0.02	∞
Power budget	0.02	R	$\sqrt{3}$	1	0.02	∞
Convergence	0.01	R	$\sqrt{3}$	1	0.01	∞
Comb. Std. Unc.					0.15	
Expanded Unc. ($k = 2$)					**0.30**	

5 Verification of the Target Values

5.1 Independent Numerical Verification

The verification was performed by the Sim4Life support group of ZMT Zurich MedTech AG, Switzerland, who performed an independent analysis of the CAD files received from the IT'IS Foundation. The results of the analysis are summarized in Table 5. The differences between the results obtained by the Sim4Life support group and the target values of Table 3 are well within the expanded uncertainty ($k = 2$) of 0.30 dB (Tables 4 and 6).

Table 5: Numerical SAR results provided by the Sim4Life support group. All results are normalized to 1 W forward power.

Frequency [MHz]	**1 g psSAR [W/kg]**	**10 g psSAR [W/kg]**	**peak SAR [W/kg]**	**20 mm SAR [W/kg]**
3900	67.6	23.3	193.7	13.3
4200	66.4	22.2	200.9	14.6
4600	66.6	21.4	219.6	16.7
4900	68.4	21.1	244.0	18.0

Table 6: Deviation of numerical SAR results provided by the Sim4Life support group of ZMT from the target values (Table 3). The maximum deviation of 0.036 dB is much smaller than the combined expanded uncertainty of the numerical evaluations ($k = 2$) of 0.42 dB.

Frequency [MHz]	**1 g psSAR Deviation [dB]**	**10 g psSAR Deviation [dB]**	**peak SAR Deviation [dB]**	**20 mm SAR Deviation [dB]**
3900	0.004	0.002	0.004	0.006
4200	−0.001	−0.001	0.000	0.000
4600	−0.007	−0.006	−0.008	−0.003
4900	−0.005	−0.004	0.036	0.032

5.2 Independent Experimental Verification

The dipoles (Figure 2), manufactured by Schmid & Partner Engineering AG (SPEAG), Switzerland, were experimentally assessed by the SPEAG calibration laboratory team using DASY52 and DASY6 systems. As mentioned in Section 3.3, the elliptical flat phantom as defined in [1] and the adapted ISO17025 accredited calibration protocol for dipoles were applied.

Figure 2: The 3900, 4200, 4600, and 4900 MHz dipoles, manufactured by SPEAG.

The measurement results are summarized in Table 7 and compared to the target values (Table 3). The uncertainty budget is evaluated according to [1] and provided in Tables 9 and 10. The differences between experimental and numerical results are well within the combined expanded uncertainty ($k = 2$) of numerical and experimental evaluation of 0.90 dB (Tables 8, 9, and 10).

Table 7: Experimental input reflection coefficients and SAR results provided by SPEAG. All results are normalized to 1 W forward power. Please note that the return losses of the numerical dipoles lower than expected, i.e., the SAR values for the experimental dipoles are expected to be higher.

Frequency [MHz]	S_{11} **[dB]**	**1 g psSAR [W/kg]**	**10 g psSAR [W/kg]**	**peak SAR [W/kg]**
3900	−23.1	72.4	25.2	201.6
4200	−22.3	68.9	23.3	198.5
4600	−25.1	69.7	23.0	214.8
4900	−23.0	70.1	22.1	228.2

Table 8: Deviation of experimental SAR results from the target values of Table 3. The maximum deviation of 0.34 dB is smaller than the uncertainty of the experimental evaluation ($k = 2$) of 0.85 dB.

Frequency [MHz]	**1 g psSAR Deviation [dB]**	**10 g psSAR Deviation [dB]**	**peak SAR Deviation [dB]**
3900	0.30	0.34	0.17
4200	0.16	0.21	−0.05
4600	0.20	0.31	−0.10
4900	0.11	0.19	−0.29

Table 9: Dipole calibration uncertainty budget for the 1 g psSAR.

Unc. component	**Tolerance [dB]**	**Prob. Distr.**	**Div.**	c_i	**Std. Unc.**	ν_i **or** ν_{eff}
Incident Power	0.15	N	1	1	0.15	∞
Probe Calibration	0.28	N	1	1	0.28	∞
Probe Isotropy	0.20	R	$\sqrt{3}$	1	0.12	∞
Probe Linearity	0.20	R	$\sqrt{3}$	1	0.12	∞
Probe Detection Limit	0.04	R	$\sqrt{3}$	1	0.03	∞
Probe Boundary Effect	0.09	R	$\sqrt{3}$	1	0.05	∞
Readout Electronics	0.01	N	1	1	0.01	∞
Probe Positioner	0.03	R	$\sqrt{3}$	1	0.02	∞
Probe Positioning	0.21	R	$\sqrt{3}$	1	0.12	∞
Extrapolation/Interpolation	0.17	R	$\sqrt{3}$	1	0.10	∞
Dipole Positioning	0.09	R	$\sqrt{3}$	1	0.05	∞
RF Ambient Conditions	0.13	R	$\sqrt{3}$	1	0.07	∞
Liquid Conductivity	0.04	R	$\sqrt{3}$	0.64	0.02	∞
Liquid Permittivity	0.25	R	$\sqrt{3}$	0.64	0.02	∞
Temp. Unc. - Conductivity	0.04	R	$\sqrt{3}$	0.60	0.02	∞
Temp. Unc. - Permittivity	0.25	R	$\sqrt{3}$	0.60	0.09	∞
Comb. Std. Unc.					0.42	
Expanded Unc. ($k = 2$)					**0.85**	

Table 10: Dipole calibration uncertainty budget for the 10 g psSAR.

Unc. component	**Tolerance [dB]**	**Prob. Distr.**	**Div.**	c_i	**Std. Unc.**	ν_i **or** ν_{eff}
Incident Power	0.15	N	1	1	0.15	∞
Probe Calibration	0.28	N	1	1	0.28	∞
Probe Isotropy	0.20	R	$\sqrt{3}$	1	0.12	∞
Probe Linearity	0.20	R	$\sqrt{3}$	1	0.12	∞
Probe Detection Limit	0.04	R	$\sqrt{3}$	1	0.03	∞
Probe Boundary Effect	0.09	R	$\sqrt{3}$	1	0.05	∞
Readout Electronics	0.01	N	1	1	0.01	∞
Probe Positioner	0.03	R	$\sqrt{3}$	1	0.02	∞
Probe Positioning	0.21	R	$\sqrt{3}$	1	0.12	∞
Extrapolation/Interpolation	0.17	R	$\sqrt{3}$	1	0.10	∞
Dipole Positioning	0.09	R	$\sqrt{3}$	1	0.05	∞
RF Ambient Conditions	0.13	R	$\sqrt{3}$	1	0.07	∞
Liquid Conductivity	0.04	R	$\sqrt{3}$	0.43	0.01	∞
Liquid Permittivity	0.25	R	$\sqrt{3}$	0.43	0.06	∞
Temp. Unc. - Conductivity	0.04	R	$\sqrt{3}$	0.40	0.01	∞
Temp. Unc. - Permittivity	0.25	R	$\sqrt{3}$	0.40	0.07	∞
Comb. Std. Unc.					0.41	
Expanded Unc. ($k = 2$)					**0.83**	

6 Conclusions

Four new dipole models for system check and validation [1] at the frequencies 3.9 GHz, 4.2 GHz, 4.6 GHz, and 4.9 GHz have been developed, and numerical SAR target values, including their numerical uncertainty budgets, have been provided. The models were validated independently by means of both numerical and experimental methods. The observed deviations were found to be much smaller than the respective expanded combined uncertainties (k=2) of both numerical evaluations of 0.42 dB, namely, the maximum deviation was 0.036 dB. The maximum deviation of the experimental evaluation was 0.34 dB whereas the combined expanded uncertainty ($k = 2$) is 0.9 dB. The CAD files of the dipoles can be provided upon request.

References

[1] IEC, *IEC/IEEE 62209-1528, CDV, Measurement procedure for the assessment of specific absorption rate of human exposure to radio frequency fields from hand-held and body-worn wireless communication devices (Frequency range of 4 MHz to 10 GHz)*, International Electrotechnical Commission (IEC), IEC Technical Committee 106, Geneva, Switzerland, 2019.

[2] Andreas Christ and Niels Kuster, "Flat phantom setup for the performance check and system validation of measurements systems according to IEEE 1528 and IEC 62 209", Tech. Rep., IT'IS Foundation for Research on Information Technologies in Society, 8004 Zürich, Switzerland, May 2002.

[3] K. S. Yee, "Numerical solution of initial boundary value problems involving Maxwell's equations in isotropic media", *IEEE Transactions on Antennas and Propagation*, vol. 14, pp. 585–589, 1966.

[4] Octave community, "GNU Octave 4.4.1", 2018.

[5] IEC/IEEE 62704-1, *Recommended Practice for Determining the Spatial-Peak Specific Absorption Rate (SAR) in the Human Body Due to Wireless Communications Devices, 30 MHz - 6 GHz — Part 1: General Requirements for using the Finite Difference Time Domain (FDTD) Method for SAR Calculations*, International Electrotechnical Commission (IEC), IEC Technical Committee 106, Geneva, Switzerland, 2017.